CHARACTERIZATION OF DIFFERENT TYPES OF Nb-AlO_x BASED JOSEPHSON TUNNEL JUNCTIONS

D.J. Adelerhof, E.P. Houwman, P.B.M. Fransen, D. Veldhuis, J. Flokstra, and H. Rogalla,

University of Twente, Faculty of Applied Physics, Low Temperature Group,
P.O.Box 217, 7500 AE Enschede, The Netherlands.

Abstract

Three types of Josephson tunnel junctions, standard Nb/Al,AlO_x/Nb, symmetric Nb/Al,AlO_x/Al/Nb, and Nb/Al, AlO_x/AlO_x/Nb containing a double oxide layer have been investigated by means of temperature dependent I-V measurements, conductance-voltage measurements, noise analysis, and Auger Electron Spectroscopy scanning across the edge of a sputtered crater profile. In standard junctions frequently small leakage currents have been observed as well as resistance fluctuations, leading to telegraph noise. Both effects can be related to the direct contact between the AlO_x and the Nb counter electrode. In none of the symmetric junctions leakage currents larger than 0.01 % of the theoretical maximum critical current have been observed. The sub-gap current of these junctions is dominated by single- and two-particle tunneling. The SNAP process, that was used to define the junction areas, affects the tunneling mechanisms below the sum-gap voltage, probably by the introduction of barrier inhomogeneities at the edges of the junctions.
The AlO_x barrier in symmetric and asymmetric junctions cannot completely be represented by a trapezoidal barrier shape. The metal-insulator interface between Al and AlO_x in both junction types is probably not very sharp, which might be due to oxygen diffusion. The metal-insulator interface between AlO_x and Nb in standard junctions can be represented by a step-wise increase of the potential barrier, indicating that this interface is very distinct. The AlO_x barrier in double oxide layer junctions is not homogeneous and probably contains low barrier channels.

Introduction

On basis of Nb and Al high quality Josephson tunnel junctions can be made [1]. The junctions are usually made of a Nb base electrode, covered by a thin Al overlayer, that is oxidized and subsequently covered by a Nb counter electrode. This type of junction is normally referred to as SNIS (S = Superconductor, N = Normal metal, I = Insulator). The SNIS configuration, however, has one mayor drawback. During oxidation of the Al overlayer, water molecules are easily adsorbed at the surface of the AlO_x. Deposition of Nb directly on top of the AlO_x leads to reactions between Nb and surface O-H groups, which may probably cause microshorts between the electrodes [2].
We have studied the effects of the AlO_x-Nb interface on the junction characteristics. Junctions of type SNIS have been compared with SNINS junctions in which an extra Al layer of various thicknesses is deposited on top of the AlO_x, prior to the Nb counter electrode deposition. Besides standard I-V measurements, conductance-voltage measurements, noise analyses, and Auger microscopy have been performed. Special attention has been paid to the presence of leaks, the shape of the potential barrier, and the occurrence of telegraph noise, which is also related to the junction configuration [3].
Finally, Josephson tunnel junctions containing a double oxide layer have been investigated. In this SNIIS type of junction the AlO_x layer is formed in a two-step process [4]. This probably affects the barrier properties of the dielectric layer.

junction	type	base electrode	oxidation pressure (mbar)	counter electrode
3d4	SNINS	Nb + 4 nm Al	267	3 nm Al + Nb
3d5	SNINS	Nb + 4 nm Al	26.7	3 nm Al + Nb
3d6	SNINS	Nb + 4 nm Al	2.67	3 nm Al + Nb
3d15	SNINS	Nb + 3 nm Al	267	2 nm Al + Nb
3d12	SNINS	Nb + 3 nm Al	267	1 nm Al + Nb
3d17	SNIS	Nb + 3 nm Al	267	Nb
3@24	SNIIS	Nb	double oxide AlO_x layer	Nb

table 1) Junction types and configuration.

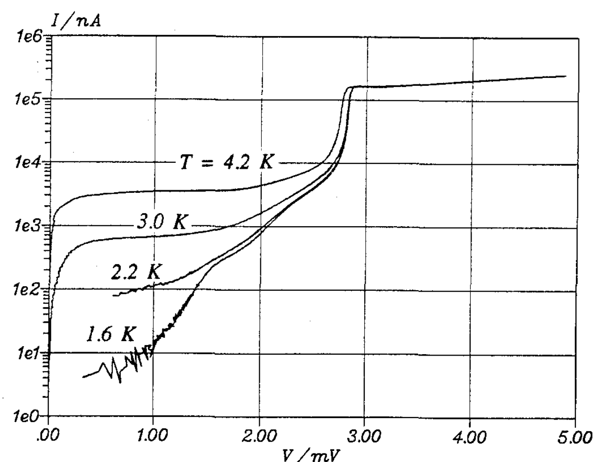

fig. 1) I-V characteristics of a 3d6 junction measured at four different temperatures.

Junction fabrication

The Nb/Al,AlO_x(/Al)/Nb trilayer is deposited in a turbo pumped vacuum system. Nb and Al films were deposited by two DC magnetron sputter guns at a rate of 200 nm/min and 22 nm/min, respectively. During sputtering the oxygen pressure was in the low 10^{-9} mbar range. The water pressure was 10^{-7}-10^{-8} mbar. The T_c of the Nb films is 9.2 K.
The trilayer configuration of the junctions is listed in table 1. The thickness of the Nb base electrodes is 300 nm. The Al overlayers were thermally oxidized in pure O_2 at 10 °C, during 1 hour. The double oxide layer of the SNIIS type junction has been formed in two steps. The Al layer was oxidized in 0.04 mbar O_2 for 15 minutes. Then a second Al layer of 10 Å was deposited and completely oxidized in 27 mbar O_2.
The junction areas (20x20, 10x10, and 5x5 μm^2 on one thermally oxidized Si wafer) were defined by SNAP (Selective Niobium Anodization Process) [5]. To complete the junctions 300 nm Nb was deposited and structured by lift-off, to form contacts with the counter electrodes.

Results on SNIS and SNINS junctions

I-V measurements

The I-V characteristics of the junctions have been obtained with help of a low noise, battery powered current source. A battery powered amplifier with an input noise of 5 nV/√Hz and a bandwidth of 80 kHz was used to amplify the voltage across the junction.
The characteristic gap and sub-gap parameters of the Josephson tunnel junctions are listed in table 2. The sum-gap voltage V_g (= $2\Delta/e$, where Δ is the superconducting gap of the electrodes at 4.2 K) is an average value of 10 junctions with a standard deviation of 0.01 mV. The theoretical maximum critical current density J_{co} is obtained from $J_{co} = I_{co}/A = \pi \cdot V_g/(4 \cdot R_N \cdot A)$, where A is the area of the junction, R_N = 4 mV/I(4 mV), and I_{co} is the critical current.
The sub-gap parameters are obtained by suppressing the zero voltage current by a magnetic field. This enabled an accurate measurement of the sub-gap current in 5x5 μm^2 junctions. In larger junctions the magnetic field induced resonant modes causing extra currents at finite voltages below V_g. This made it very difficult to measure the sub-gap current accurately.
With our sample holder we could measure four 5x5 μm^2 junctions

junction	type	Gap parameters		Sub-gap parameters				Barrier parameters		
		V_g (mV)	J_{co}	I_1/I_{co} (%)		I_2/I_{co} (%)		d	ϕ_{BE}	ϕ_{CE}
		4.2 K	(A/cm^2)	4.2 K	± 1.6 K	4.2 K	± 1.6 K	(Å)	(eV)	(eV)
3d4	SNINS	2.76	44			3.2 - 3.5		9.1	1.66	1.72
3d5	SNINS	2.77	162	3.0 - 3.2	0.014 - 0.13	3.9 - 4.3	0.68 - 1.1	8.6	1.49	1.59
3d6	SNINS	2.76	595	3.0 - 3.1	0.010 - 0.015	3.8 - 3.8	0.65 - 0.71	8.0	1.30	1.50
3d15	SNINS	2.77	40	2.8 - 3.5	0.010 - 0.082	3.2 - 3.7	0.41 - 0.90	9.7	1.45	1.50
3d12	SNINS	2.83	36	2.7 - 2.9	0.034 - 0.042	3.4 - 4.4	0.62 - 1.6	10.1	1.24	1.50
3d17	SNIS	2.78	110	3.3 - 4.9	0.046 - 1.7	5.1 - 7.0	1.7 - 3.7	8.8	1.7	1.5
3@24	SNIIS	2.80	48			5.4 - 5.9		-	-	-

table 2) Junction parameters. The values of V_g are average values of 10 junctions with different areas. The sub-gap parameters are minimum and maximum values, as obtained from measurements on 4 junctions of 25 μm^2.

after one cool-down. The measured values of I_1/I_{co} (I_1 = I at V = 1 mV) and I_2/I_{co} (I_2 = I at V = 2 mV) are all between the minimum and maximum values listed in table 2. The values of I_2/I_{co} of all SNINS junctions we measured indicate, that the quality of the junctions is very good. The quality parameter V_m (= 2 mV·I_{co}/I_2) ranges between 45 and 63 mV, which is very high, although higher values, up to 80 mV, have been reported [1].

In fig. 1 the I-V characteristics at four different temperatures of one of the 3d6 SNINS junctions are shown. This figure shows, that at 4.2 K the sub-gap currents I_1 and I_2 are of the same order of magnitude. At this temperature I_1 and I_2 are dominated by single-particle tunneling. When the temperature decreases, I_2 reduces until T ≈ 2 K. Below this temperature I_2 changes only very slightly. I_1, however, still decreases significantly at temperatures below 2 K. In fact, even at 1.6 K the current at 1 mV is strongly temperature dependent. The differences in the minimum values of I_1/I_{co} at 1.6 K as listed in table 2 are due to this dependence, since the lowest temperature that was achieved differed within 0.1 K. The difference between I_2 and I_1 remains about constant at cooling down.

From fig. 1 it can be seen, that the difference between I_1 and I_2 is related to an onset of extra tunneling at $1/2V_g$. This onset has been observed in all SNINS junctions. We think, that this is due to two-particle tunneling, as proposed by J.R. Schrieffer and J.W.Wilkins [6]. They showed, that this tunneling mechanism causes a sharp onset of the sub-gap current at V = 1/2 V_g (in case of identical superconducting electrodes), and a strongly increasing current at higher voltages. The temperature dependence of two-particle tunneling is small, which explains the constant difference between I_2 and I_1, at cooling down. Two-particle tunneling was not observed in the measurements in ref. 1, which probably explains the higher value of V_m as compared to the values, that we have obtained.

The I-V characteristics of some junctions also showed an onset of extra tunneling at $V_g/3$, which indicates the occurrence of three-particle tunneling. The spread in values of the sub-gap currents at 1.6 K between junctions on the same wafer is mainly due to this effect. It is not yet clear, why this extra tunneling at $V_g/3$ is not the same in junctions, that were made simultaneously on one wafer, and thus are expected to behave identical.

Another interesting effect is, that in junctions with larger areas I_2/I_{co} is always smaller than in 5x5 μm^2 junctions. In junctions of 20x20 μm^2 values of I_2/I_{co} = 0.2 % at 1.6 K have been obtained. The anodized Nb that surrounds the Nb/Al trilayer apparently affects the sub-gap current. Possibly, the anodized Nb behaves as a low barrier contact between the electrodes. It's also thinkable, that stress is built up at the edges of the AlO_x during anodization, possibly causing barrier inhomogeneities.

In none of the SNINS junctions we could observe leakage currents larger than 10^{-4}·I_{co} at 1 mV. Leakage currents show up as temperature independent sub-gap currents, increasing linearly with voltage. Single- and two-particle tunneling dominate the sub-gap currents of the SNINS junctions. In some of the junctions three-particle tunneling also contributes to the current below V_g.

The 5x5 μm^2 SNIS junctions listed in table 2 contained micro-shorts in three out of four junctions. The 3d17 junctions with larger areas (not shown in table 2) made on the same wafer, all

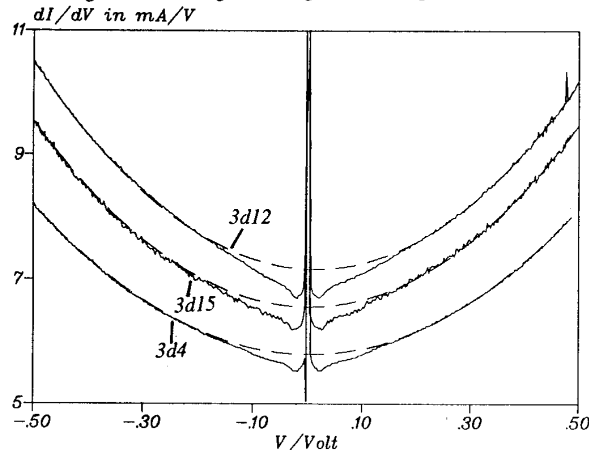

fig. 2) Conductance vs voltage for three different SNINS junctions. The upper curve is from a 3d12 junction and has been shifted up with 2 mA/V, for clarity. The middle curve, with an offset of 1 mA/V, is measured for a 3d15 junction. The lower curve is from a 3d4 junction and has no offset. All curves were measured at 4.2 K. The area of the junctions is 25 μm^2. The dashed curves are theoretical fits. A positive voltage corresponds to a positively biased counter electrode.

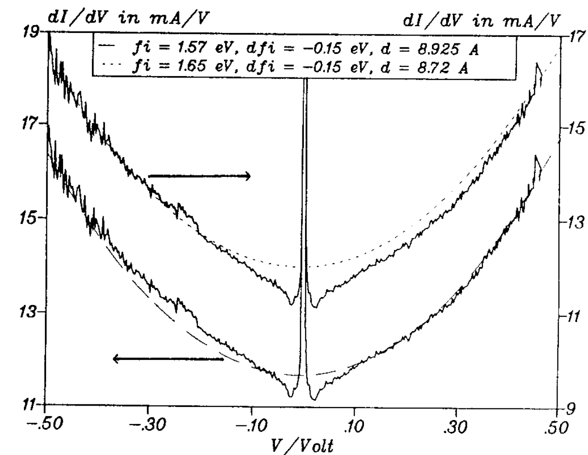

fig. 3) Conductance vs voltage for a 3d17 SNIS junction of 25 μm^2, measured at 4.2 K. The theoretical curves (dashed and dotted curves) have been fitted with the negative voltage range and with the positive voltage range of the experimental curves. The parameters obtained from both fits are shown in the legend (fi = Φ, dfi = ΔΦ). The noise at V < -0.2 V is due to resistance fluctuations.

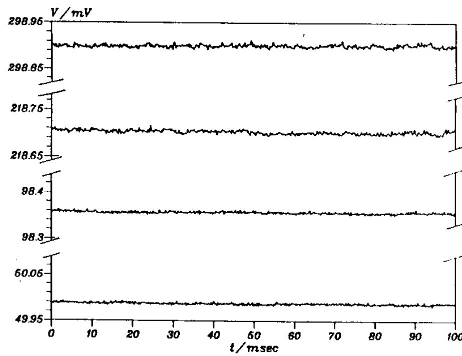

fig. 4a) Voltage-time traces of a 3d4 SNINS junction of 25 μm^2, measured at 4.2 K.

had leakage currents. More generally, it's our experience, that SNIS junctions frequently contain microshorts. These results support the hypothesis in ref. 2, that due to reactions between Nb and H_2O, microshorts between the electrodes can occur. The one junction without observable leakage currents had similar sub-gap I-V characteristics as the SNINS junctions, resulting in $I_1 = 4.6 \cdot 10^{-4} \cdot I_{co}$ at 1.6 K.

The effects of an extra Al layer on V_g can be seen by comparing junctions 3d4, 3d15, and 3d12. The superconducting gap increases slightly if the thickness of the normal conducting Al layers is reduced. The influence of the Al on the sum-gap voltage is, however, very small.

Conductance-voltage measurements

With help of a standard lock-in technique dV/dI was measured as function of the voltage across the junction. The induced voltage modulation was typically about 0.5 mV (peak-peak). The output signal of the lock-in amplifier was recorded by computer with help of a 16 bits IOtech ADC488/8S A/D converter, in which the converter is optically isolated from the digital circuitry and the IEEE bus.

The experimental σ-V curves have been fitted by a theoretical conductance-voltage dependence based on a trapezoidal barrier shape [7]. In this model the Metal-Insulator-Metal (MIM) junction is represented by a potential barrier with average barrier height $\bar{\phi}$ ($= 0.5 \cdot (\phi_{Base\ Electrode} + \phi_{Counter\ Electrode})$), asymmetry $\Delta\phi$ ($= (\phi_{CE} - \phi_{BE})$) and thickness d, that impedes the electron flow between the two metallic electrodes.

The σ-V characteristics were usually measured at 4.2 K. In order to check whether tunneling is the dominant electron flow mechanism, the σ-V characteristics of a few junctions have also been determined at 77 K. Apart from the superconducting tunneling effects, the characteristics did not change, as expected in case of electron tunneling.

The barrier parameters obtained from fitting the measured characteristics with theory are listed in table 2. In fig. 2 and 3 experimental conductance-voltage curves of 3 different SNINS junctions (3d4, 3d15, and 3d12) and 1 SNIS junction (3d17) are shown. It can be seen, that the σ-V curves of the symmetrical SNINS junctions can be fitted by the (dashed) theoretical curves at voltages above 200 mV. Below 200 mV, the experimental curve deviates from the theoretical curve. Apparently, the AlO_x barrier in SNINS junctions cannot completely be represented by a trapezoidal barrier shape. This probably also explains the differences between the barrier parameters of junctions 3d4, 3d15, and 3d12. One should expect that the barrier shapes of the AlO_x are the same, since the thermal oxidation conditions of these junctions are identical.

The σ-V characteristic of the SNIS junction in fig. 3 can also not be fitted completely with a theoretical curve. The experimental curve has been fitted in two ways. In one case, the barrier parameters are adjusted to obtain the best fit for V < 0, which corresponds to a positively biased base electrode. Below V = -200 mV the theoretical curve coincides with the experimental curve. At voltages between 0 and -200 mV, however, the two curves deviate in a way very similar to the deviation observed in SNINS junctions. This was to be expected, since the Nb/Al base electrode configuration in both junctions is identical. The other

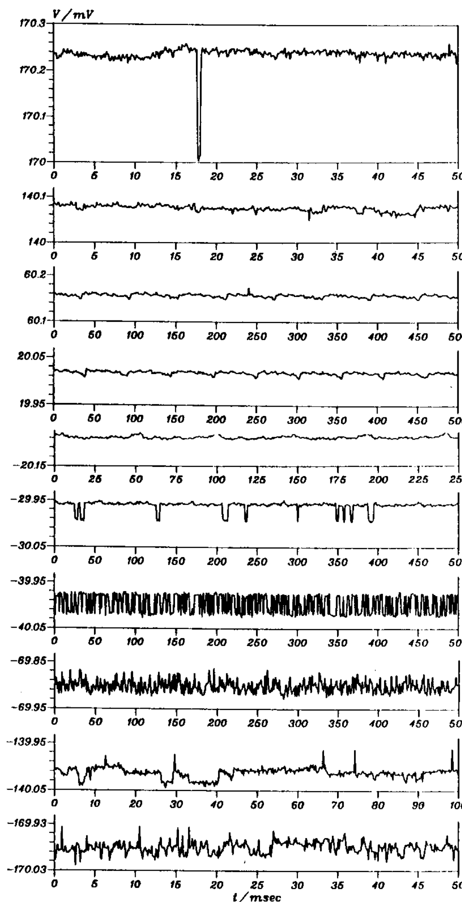

fig. 4b) Voltage-time traces of a 3d17 SNIS junction of 25 μm^2, measured at 4.2 K.

fit is obtained from fitting the positive voltage side of the experimental curve. In this voltage range the conductance curve can almost completely be described by the trapezoidal barrier shape model. Apparently, the metal-insulator interface between the AlO_x and the Nb counter electrode is quite distinct.

Noise measurements

The noise properties of SNINS 3d4, 3d15, 3d12, and SNIS 3d17 junctions at 4.2 K have been investigated at voltages up to 300 mV. The voltage-time traces were recorded by computer. The use of the computer did not affect the observed noise properties.

Voltage-time traces of a 3d4 SNINS and a 3d17 SNIS junction are depicted in figs. 4a and 4b, respectively. The traces of the 3d4 junction do not show any telegraph noise at voltages between -300 and 300 mV. This behaviour is typical for all 3d4 SNINS junctions we investigated. The voltage-time traces of the SNIS junction, however, do show telegraph noise between -30 and -50 mV, as well as a more complicated noise at more negative voltages. At +170 mV some voltage switching with $\Delta V \approx 0.2$ mV can be observed. The voltage-time traces of all SNIS junctions are more or less similar to those shown in fig. 4b.

In junctions 3d15 and 3d12, in which the second Al layer is thinner than in 3d4, a 'telegraph noise-like' noise behaviour is observed, although to a lesser extent than in SNIS junctions.

These measurements strongly suggest, that the Nb-AlO_x interface plays an important role in the introduction of noise sources in SNIS junctions. In junctions 3d15 and 3d12 the second Al layer is apparently too thin to cover the AlO_x completely and contacts between the Nb counter electrode and the AlO_x still occur.

The occurrence of telegraph noise in small junctions is usually explained by the presence of localized states in the barrier, where electrons can be trapped or released, thereby introducing a

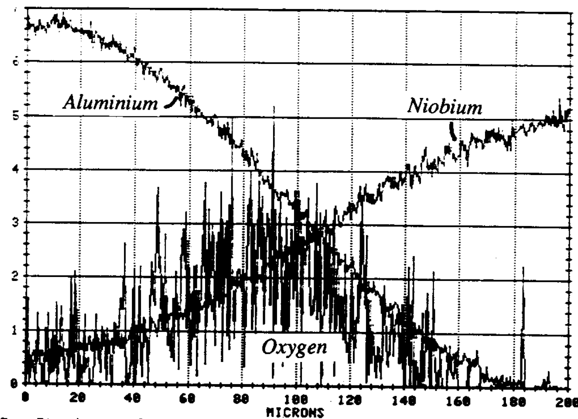

fig. 5) Auger line profile across the interface of a thermally oxidized Al layer and a Nb layer. The line scan was made across the edge of a crater. The overlap of the different elements is due to the information depth. See text

discrete change of the junction resistance [8]. The voltage dependence of this mechanism comes in through the activation energy. With respect to the junctions investigated in this study, this would imply, that due to the direct contact between Nb and AlO_x, localized states are introduced in the barrier. The presence of localized states at one side of the barrier would also explain the asymmetric voltage dependence of the observed noise. The oxidation of Nb at the Nb-AlO_x interface can give rise to the formation of localized states in the barrier [2,9].

Scanning Auger Microscopy

With help of Auger line profiles information about the AlO_x-Nb interface has been obtained. For this purpose, a special sample was prepared. On top of a Si wafer 20 nm Al was deposited. The Al surface was thermally oxidized in 267 mbar pure oxygen for 1 hour, and subsequently covered by 300 nm of Nb.
In a UHV system (background pressure: $3 \cdot 10^{-10}$ mbar) a crater profile was etched in this sample, with help of an Ar ion beam. Directly after this etching Auger line scans were made across the edge of the crater profile. These scans had to be made within 1 minute, to avoid that the Al and Nb were covered with residual gasses present in the chamber. Nb preferentially adsorbed CO and CO_2, Al mainly adsorbed H_2O. The angle between the sample surface and the surface of the crater edge equals $\approx$ 0.06 degrees. The information depth is about 60 Å, which is three times the inelastic mean free path of the Auger electrons.
In fig. 5 an Auger line scan across the AlO_x-Nb interface is shown. It can be seen, that oxygen is always detected together with Al. There is no position where Nb and O are detected in absence of Al, which indicates that diffusion of oxygen into the Nb hardly occurs. The decay of Nb, which is relatively long as compared to the Al decay, may suggest that Nb has diffused into the AlO_x layer. It is, however, very likely, that this long decay is caused by sputter artifacts.

Results on double oxide SNIIS junctions

The conductance-voltage characteristics of double oxide SNIIS junctions can not be fitted by the theoretical curves, as can be seen in fig. 6. At low voltages the conductance is almost the same as in junctions of type 3d4, but above ± 10 mV dI/dV strongly increases. The experimental curve in this figure is typical for all junctions of this type.
In SNIIS junctions the barrier shape is apparently not trapezoidal. The σ-V curves can be explained by the presence of low barrier channels in the AlO_x, that become highly conductive at voltages above 10 mV. This indicates, that the second Al layer does not cover the AlO_x completely. The noise measurements on SNINS junctions with variable thicknesses of the second Al layer did already suggest that.
The gap and sub-gap parameters of SNIIS junctions are comparable to standard SNIS junctions.

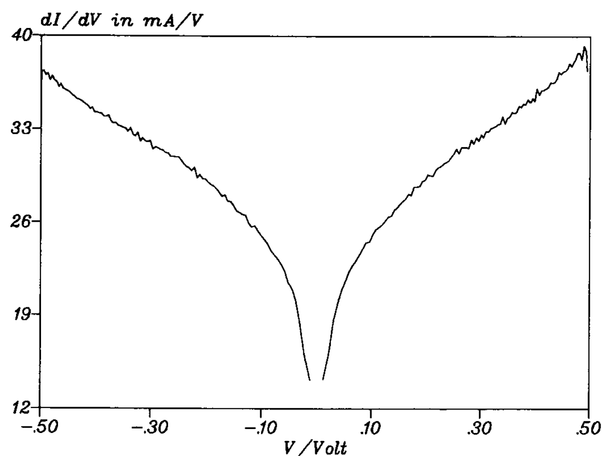

fig. 6) Conductance vs voltage of a 3@24 SNIIS junction of 25 μm^2, measured at 4.2 K.

Conclusions

High quality SNINS Nb/Al Josephson tunnel junctions with leakage currents below 0.01 % of the zero voltage current have been made. The reproducibility of the fabrication process is very good. The sub-gap tunneling current in these junctions is dominated by single- and two-particle tunneling. In some junctions also three-particle tunneling was observed.
The occurrence of two- and three-electron tunneling indicates, that the barrier in the SNINS is inhomogeneous. The measurements suggest, that the anodized Nb, that surrounds the junctions, affects the sub-gap current. It is very likely, that the SNAP process, that was used to define the area of the junctions, causes barrier inhomogeneities at the edges of the junction. It may be expected, that SNEP (Selective Niobium Etching Process) affects the sub-gap current to a lesser extent, which would explain the high value of V_m in ref. 1.
The AlO_x barrier in SNINS junctions cannot completely be represented by a trapezoidal barrier shape. It is possible, that due to oxygen diffusion, the potential barrier at the Al-AlO_x interface increases rather smoothly, instead of step-wise. It is not yet clear, whether barrier inhomogeneities at the edges of the junctions affect the σ-V characteristics.
In standard SNIS junctions frequently microshorts are present and resistance fluctuations occur, which both can be related to the direct contact between the AlO_x and the Nb counter electrode. M. Ronay and E.-E Latta have proposed a mechanism, that can very well account for both effects [2]. They suggested, that during oxidation of Al the pores of the AlO_x become sealed by surface O-H groups. When Nb is deposited on top of the AlO_x the O-H groups react with Nb to form NbO, thereby opening up the pores and causing microshorts. We think, that due to this process also localized states are formed at the AlO_x-Nb interface. These localized states may give rise to resistance fluctuations.
The metal-insulator transition between the AlO_x and the Nb is sharp, as was concluded from σ-V measurements and supported by Auger Electron Spectroscopy.
The AlO_x barrier in double oxide layer SNIIS Nb/Al junctions is not homogeneous and probably contains low barrier channels. However, good superconducting tunneling properties can be obtained. This offers the possibility to make good quality junctions with high normal resistance. The quality might even be improved by using an SNIINS configuration.

References

(1) A.W. Lichtenberger *et al.*, *IEEE Trans. Mag.* **25**, 1247, 1989.
(2) M. Ronay and E.-E. Latta, *Phys. Rev. B* **27**, 1605, 1983.
(3) D.J. Adelerhof *et al.*, *Phys. B* **165&166**, 1581, 1990.
(4) E.P. Houwman *et al.*, *J. Appl. Phys.* **67**, 1992, 1990.
(5) H. Kroger *et al.*, *Appl. Phys. Lett.* **39**, 280 1981.
(6) J.R. Schrieffer *et al.*, *Phys. Rev. Lett.* **10**, 17, 1963.
(7) W.F. Brinkman *et al.*, *J. Appl Phys.* **41**, 1915, 1970.
(8) C.T. Rogers *et al.*,*Phys. Rev. Lett.* **53**, 1272, 1984.
(9) J. Halbritter, *IEEE Trans. Mag.* **Mag-19**, 799, 1983.